IEEE TRANSACTIONS ON AEROSPACE AND ELECTRONIC SYSTEMS, Volume 57, Number 5, October 2021, pp. 3004-3014
DOI:10.1109TAES.2021.3067656

An Improvement in Three-Dimensional Pure Proportional Navigation Guidance

Hyo-Sang Shin and Ke-Bo Li

Abstract

This paper proposes an improved version of 3D pure proportional navigation (PPN) against a manoeuvring target. The main research hypothesis is that the performance of 3D PPN can be improved by properly selecting the direction of the guidance command as there exists an infinite number of potential directions complying with the PPN concept in 3D space. Analysis on the relative motion confirms the validity of the hypothesis and leads to the development of a new guidance algorithm. Unlike traditional 3D PPN, the guidance algorithm developed adapts the direction, but maintains the magnitude of the commanded acceleration proportional to only the line-of-sight (LOS) rate. The validity and performance of the proposed guidance algorithm are investigated through theoretical analysis and numerical simulations.

Index Terms

3D PPN, manoeuvring target, direction of commanded acceleration, relative motion analysis

I. Introduction

Pure proportional navigation (PPN) guidance law [1]–[6] is a major class of proportional navigation (PN) guidance laws and mainly used for endo-atmospheric interception, whereas true proportional navigation (TPN) guidance law [7]–[9] is another major PN class that is commonly used for exo-atmospheric interception. The commanded acceleration vector of PPN is perpendicular to the interceptor's velocity vector and its magnitude is proportional to the line-of-sight (LOS) angular rate. PPN is preferred over many other guidance laws mostly thanks to its robustness and practicality [10]. Implementation of PPN mainly requires the measurement of LOS rate, which is generally available from the gimballed seeker system on the interceptor.

It is known that PPN provides excellent capturability against non-manoeuvring target for endo-atmospheric interception [6]. The LOS rate and commanded acceleration of PPN are continuously decreasing during the guidance process, and the capture region is extremely large. However, if the target is manoeuvring with large acceleration, performance of PPN might be significantly degraded. Many researchers have investigated the performance of PPN against manoeuvring targets using linear or nonlinear methods. For example, Shukla and Mahapatra [11] extended

H.-S. Shin is with the Institute of Aerospace Sciences, SATM, Cranfield University, College Road, Cranfield, Bedfordshire, MK43 0AL, United Kingdom.

K.-B. Li is Department of Aerospace, College of Aerospace Science and Technology, National University of Defense Technology, Changsha, Hunan, 410073, China

their quasi-linearisation method of PPN [12] to the scenario of manoeuvring target interception and obtained closed-form solutions of trajectory parameters. Gulman [11], [13] presented some qualitative results of PPN against constantly manoeuvring targets based on his previous qualitative analysis approach [3]. Ghawghawe and Ghose [14] study the capturability of PPN against an arbitrarily manoeuvring target with time-varying normal acceleration by utilising Guelman's approach [3], [11], [13]. Based on the Lyapunov-like approach [15]–[17], Oh and Ha [18], [19] presented the capture condition and the upper-bound of commanded acceleration of PPN against an arbitrarily manoeuvring target. Recently, K. B. Li *et al.* [20] restudied the results of [17]–[19] and obtained more general conditions.

These studies confirm that performance of PPN is degraded if the target manoeuvres. Hence, for improving the performance of endo-atmospheric interceptors against manoeuvring targets, there have been numerous guidance algorithms developed, based on different types of modern control theories such as optimal guidance laws [21], [22], sliding mode guidance laws [23]–[27] and differential game guidance laws [28], [29]. However, these algorithms tend to require additional information, e.g. time-to-go, relative range, or even the target acceleration, for obtaining commanded accelerations. This might increase the complexity of the guidance system and also could even result in some robustness issue.

This paper aims to develop a new guidance algorithm to enhance the performance of endo-atmospheric interceptors against manoeuvring targets. Thanks to the widely accepted advantages, this paper will exploit the main concepts of PN in the development. Since the target with high acceleration manoeuvres could cause a significantly change of the engagement plane, it is necessary to cope with the 3D engagement problem even for homing guidance.

Unlike in 2D space, determination of the guidance command direction becomes important in 3D space. In 2D space, there exists one direction that is perpendicular to the velocity vector of the interceptor and able to reduce the LOS rate at the same time. On the other hand, there exist an infinite number of potential directions of the guidance command in 3D space as a plane is perpendicular to the velocity vector. The direction of 3D PPN is determined by the cross product of the LOS angular velocity and interceptor's velocity [1], [5], [6]. Some modern advanced guidance laws also adopt the direction of the guidance command from 3D PPN, e.g. [30]. Another representative approach is to split the 3D space into two 2D engagement planes, i.e. pitch and yaw planes. The guidance commands in the two planes are computed by 2D PPN and the direction of the guidance command in 3D space is then constructed from the vector sum.

There have been attempts to introduce the differential geometric curve theory into the 3D guidance law design, which have led to various 3D differential geometric guidance laws (DGGLs) [31]–[34]. DGGLs were claimed to provide excellent guidance performance against manoeuvring targets. It is worth noting that such guidance laws produce guidance command formations and directions, different from traditional 3D PPN. The results of DGGLs indicate that the difference in the command formation and direction might play a crucial role in improving the guidance performance. However, up to the best of our knowledge, there have been no studies analysing the effectiveness of command directions on the guidance performance in 3D space.

Therefore, this paper first focuses on performing relative motion analysis between the interceptor and the target to find an efficient direction of the guidance command . The efficient direction of the guidance command is defined

as the direction that enables efficient reduction of the *zero-effort miss (ZEM)*. Note that ZEM is the nominal miss distance determined without considering the accelerations. It is widely accepted that target interception can be achieved by efficiently reducing *ZEM*. This paper then focuses on developing a new 3D PPN, named Improved Pure Proportional Navigation (IPPN), by leveraging the efficient direction found. The calculation of the new command direction requires the same measurement information of traditional 3D PPN, which enables IPPN to keep the main advantages of 3D PPN, namely practicality and robustness. Another main modification from 3D PPN is that IPPN maintains the magnitude of the guidance command proportional only to the LOS rate. This will allow the proposed guidance law to efficiently stabilise the LOS rate.

The validity of our main arguments is examined by theoretically analysis. The analysis is based on the Lyapunov-like approach [15], [17]. The analysis results indicate that if the navigation gain in IPPN is properly selected, then our arguments can be validated. The performance of the proposed guidance algorithm is investigated and compared with that of 3D PPN through numerical simulations. The simulation results confirm that IPPN reduces the ZEM and stabilise the LOS rate in a more efficient way, compared with 3D PPN. Consequently, the IPPN guidance law can significantly improve guidance performance.

The remainder of the paper is organised as follows. Section II introduces preliminaries and the 3D relative kinematic equation set established in the LOS rotation coordinate system. Section III, conducts relative motion analysis to investigate efficient directions of the guidance command and develops the IPPN guidance law. The validity of the main arguments are theoretically analysed in Section IV and numerical simulation results are provided in section V. Finally, conclusions are offered in section VI.

II. Preliminary

Traditionally, the 3D pursuit is handled by constructing two independent guidance laws in the pitch and yaw planes of the missile and taking their cross-coupling effect into account. This approach might complicate the description of the relative motion due to the cross-coupling effect and introduce some auxiliary variables to the guidance law. Establishing the kinematic equations in LOS rotating coordinate (LRC) could ease the complexity in the description of the 3D relative motion [35]–[37]. The relative motion in the LRC system can be divided into two decoupled submotions: 1) the relative motion in the engagement plane spanned by the relative position and velocity vectors and 2) the rotation of this plane. This paper will use these kinematic equations in developing an improved PPN guidance law.

In this paper, we consider the 3D engagement problem in which a missile guided by PPN pursues an arbitrarily manoeuvring target with time-varying normal acceleration. Like in numerous previous studies [1]–[3], [13], [17], [18], for the simplicity of the performance analysis, this paper assumes that:

A1) The missile and target are considered as point masses moving in 3D space;

A2) Compared with the resulting overall guidance loop, the autopilot and the seeker dynamics are fast enough to be neglected;

A3) The angle of attack (AOA) and angle of sideslip (AOS) of the missile are small enough to be neglected;

A4) The speeds of missile and target are constant.

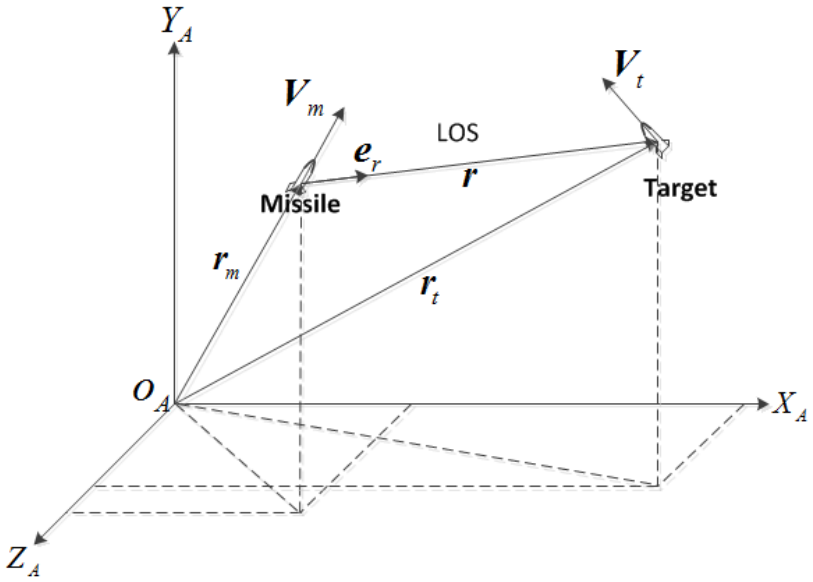

Fig. 1: Three-dimensional engagement geometry.

A5) The speed of missile is greater than that of the target.

It is further assumed that the earth is non-rotating. Note that PPN guidance is widely used in homing guidance and homing guidance phase is relatively short. Therefore, in homing guidance, the constant speed assumption with the non-rotation earth one could be acceptable. One could argue that only 2D engagement geometry could be considered in homing guidance. However, since the engagement plane could be significantly changing when the target is manoeuvring with high acceleration, coping with 3D engagement problem is necessary even for homing guidance.

Fig. 1 depicts 3D pursuit geometry. In Fig. 1, the frame $O_A - X_A Y_A Z_A$ denotes the inertial launch frame, which is fixed and centred at the launch site. The origin O_A is fixed at the launch point, the X_A axis lies in the horizontal plane and points to the launch direction of the missile, while the Y_A axis is aligned with the local orthogonal direction of the launch point, and the Z_A axis completes a right-handed frame with the other two axes. The position vectors of the missile and target are denoted as $\boldsymbol{r}_m$ and $\boldsymbol{r}_t$, respectively. The relative position vector $\boldsymbol{r}$ is given by

$$\boldsymbol{r} = \boldsymbol{r}_t - \boldsymbol{r}_m \tag{1}$$

LOS is defined as the direction pointed from the missile to the target, namely,

$$\boldsymbol{e}_r = \boldsymbol{r}/r \tag{2}$$

where r is the relative range.

The relative velocity can be decomposed into two major components. The first one is the velocity component and is called *closing velocity*:

$$\boldsymbol{v}_r = v_r \boldsymbol{e}_r \tag{3}$$

where v_r denotes the closing speed which is equal to $\dot{r}$. The second component is perpendicular to the LOS and is called *vertical relative velocity* which is given by:

$$\begin{cases} \boldsymbol{v}_\theta = \boldsymbol{\omega}_s \times \boldsymbol{r} = v_\theta \boldsymbol{e}_\theta \\ v_\theta = r\omega_s \end{cases} \tag{4}$$

where $\boldsymbol{\omega}_s$ denotes the angular velocity of $\boldsymbol{r}$, $\boldsymbol{e}_\theta$ is the unit vector along $\boldsymbol{\omega}_s \times \boldsymbol{r}$ and ω_s is the angular speed of the LOS vector. The angular velocity of LOS, $\boldsymbol{\omega}$ and its direction $\boldsymbol{e}_\omega$ can be represented as:

$$\begin{aligned} \boldsymbol{\omega}_s &= \omega_s \boldsymbol{e}_\omega \\ \boldsymbol{e}_\omega &= \boldsymbol{e}_r \times \boldsymbol{e}_\theta \end{aligned} \tag{5}$$

Note that, from its definition, ω_s is non-negative.

LRC is defined as the rotation coordinate frame whose axes are along the unit vectors of $(\boldsymbol{e}_r, \boldsymbol{e}_\theta, \boldsymbol{e}_\omega)$. The angular velocity, $\boldsymbol{\omega}$, of the rotating axes $(\boldsymbol{e}_r, \boldsymbol{e}_\theta, \boldsymbol{e}_\omega)$, can be represented as:

$$\boldsymbol{\omega} = \omega_s \boldsymbol{e}_\omega + \boldsymbol{\Omega}_s = \omega_s \boldsymbol{e}_\omega + \Omega_s \boldsymbol{e}_r \tag{6}$$

where $\boldsymbol{\Omega}_s$ is the component of $\boldsymbol{\omega}$ along $\boldsymbol{r}$, and Ω_s denotes the angular speed of the engagement plane. Then, the following property holds [35]–[37]:

$$\begin{cases} \dot{\boldsymbol{e}}_r = \omega_s \boldsymbol{e}_\theta \\ \dot{\boldsymbol{e}}_\theta = -\omega_s \boldsymbol{e}_r + \Omega_s \boldsymbol{e}_\omega \\ \dot{\boldsymbol{e}}_\omega = -\Omega_s \boldsymbol{e}_\theta \end{cases} \tag{7}$$

Given Eqn. (7), the second time derivative of $\boldsymbol{r}$ is obtained as:

$$\boldsymbol{a} =: \ddot{\boldsymbol{r}} = \left(\ddot{r} - r\omega_s^2\right) \boldsymbol{e}_r + \left(r\dot{\omega}_s + 2\dot{r}\omega_s\right) \boldsymbol{e}_\theta + r\omega_s\Omega_s \boldsymbol{e}_\omega \tag{8}$$

where $\boldsymbol{a}$ denotes the relative acceleration of the missile w.r.t the target. The relative kinematic equation set in rotating LOS frame is then given by:

$$\begin{cases} \ddot{r} - r\omega_s^2 = a_{tr} - a_{mr} \\ r\dot{\omega}_s + 2\dot{r}\omega_s = a_{t\theta} - a_{m\theta} \\ r\omega_s\Omega_s = a_{t\omega} - a_{m\omega} \end{cases} \tag{9}$$

where a is the magnitude of the acceleration and subscripts r, θ, ω on variables represent projections of those variables onto the three axes of $(\boldsymbol{e}_r, \boldsymbol{e}_\theta, \boldsymbol{e}_\omega)$. Variables with subscripts m and t imply those variables of the missile and target. The first two equations in Eqn. (9) in describe the relative motion in the engagement plane and the third equation represents the rotational principle of the engagement plane. As shown in Eqn. (9), the first two equations can be decoupled with the third one. For more details, the reader is referred to [35]–[37].

It is assumed that the target acceleration is applied perpendicular to its velocity vector and its magnitude is assumed to be bounded from above, i.e.:

A6)

$$a_t(t) \leq \alpha, \quad \forall t \geq t_0 (= 0) \tag{10}$$

where a_t denotes the magnitude of the target acceleration and $\alpha(>0)$ the upper bound of magnitude of the target acceleration. Throughout the paper, subscript 0 on variables means the initial condition of those variables.

θ_m and θ_t define the geometric relationship between the velocity directions and $\boldsymbol{e}_r$, as represented in the following equations:

$$\begin{cases} \boldsymbol{t}_m \cdot \boldsymbol{e}_r = \cos\theta_m \\ \boldsymbol{t}_t \cdot \boldsymbol{e}_r = \cos\theta_t \end{cases} \tag{11}$$

If $\cos\theta_m$ is larger than zero, the missile is flying towards the target. Otherwise, the missile is moving away from the target. In this paper, we mainly discuss the situation where the missile is initially flying towards the target like in homing guidance, that is,

A7)

$$\boldsymbol{t}_{m0} \cdot \boldsymbol{e}_{r0} = \cos\theta_{m0} > 0 \qquad \text{or} \qquad \theta_{m0} \in \left[0, \frac{\pi}{2}\right) \tag{12}$$

Now, let us define $\boldsymbol{m}$ and $\boldsymbol{t}$ as:

$$\begin{cases} \boldsymbol{m} =: \boldsymbol{t}_m - (\boldsymbol{t}_m \cdot \boldsymbol{e}_r)\,\boldsymbol{e}_r \\ \boldsymbol{t} =: \boldsymbol{t}_t - (\boldsymbol{t}_t \cdot \boldsymbol{e}_r)\,\boldsymbol{e}_r \end{cases} \tag{13}$$

Since, from the definition, $\theta_m, \theta_t \in [0,\ \pi]$, we have:

$$\begin{cases} |\boldsymbol{m}| = \sin\theta_m \\ |\boldsymbol{t}| = \sin\theta_t \end{cases} \tag{14}$$

According to the definitions, $\boldsymbol{m}$ and $\boldsymbol{t}$ lie in the plane vertical to LOS, which was called "the LOS plane" in [17]. The angle between $\boldsymbol{m}$ and $\boldsymbol{t}$ is denoted as Θ and is an element of the set of $[0, \pi]$in this paper . Then,

$$\cos\Theta = \frac{\boldsymbol{m} \cdot \boldsymbol{t}}{|\boldsymbol{m}||\boldsymbol{t}|} = \frac{\boldsymbol{t}_m \cdot \boldsymbol{t}_t - \cos\theta_m \cos\theta_t}{\sin\theta_m \sin\theta_t} \tag{15}$$

From the definitions and assumptions made, the following kinematics can be obtained:

$$\dot{r} = \boldsymbol{v} \cdot \boldsymbol{e}_r = v_m\left(\rho \boldsymbol{t}_t \cdot \boldsymbol{e}_r - \boldsymbol{t}_m \cdot \boldsymbol{e}_r\right) = v_m\left(\rho\cos\theta_t - \cos\theta_m\right) \tag{16}$$

$$v_\theta = r\omega_s = \boldsymbol{v} \cdot \boldsymbol{e}_\theta = v_m\left|\rho\boldsymbol{t} - \boldsymbol{m}\right| \tag{17}$$

where $\rho = v_t/v_m$. Note that from the assumption A5), we have $0 < \rho < 1$.

III. New 3D PPN

A. Analysis of Relative Motion Based on ZEM

Concerning the interception problem, the theoretical goal is to reduce the relative range to zero. However, it could be difficult to achieve the goal in practice due to various reasons such as noise, uncertainties, and disturbances. Therefore, achieving the minimum miss distance is widely accepted as a practical goal of many guidance laws. Note that miss distance is defined as the minimum distance between the missile and target during the engagement. As discussed in Introduction, there exists a nominal miss distance determined without considering the accelerations, which is thus called *ZEM*. Generally, guidance considers the accelerations as the control variable of *ZEM* and the

guidance problem is to determine this control variable to drive *ZEM* to an acceptable range, near to zero, during the engagement. Given $\dot{r} < 0$, *ZEM* can be approximated as:

$$ZEM = \frac{r^2 \omega_s}{|v_r|} \tag{18}$$

The first time derivative of *ZEM* is obtained as:

$$\frac{d\,ZEM}{d\,t} = \frac{r^2(\ddot{r}\omega_s - \dot{r}\dot{\omega}_s)}{\dot{r}^2} - 2r\omega_s \tag{19}$$

From the first two equations of Eqn. (9), we have:

$$\begin{cases} \ddot{r} = a_{tr} - a_{tm} + r\omega_s^2 \\ \dot{\omega}_s = \dfrac{a_{t\theta} - a_{m\theta} - 2\dot{r}\omega_s}{r} \end{cases} \tag{20}$$

Substituting Eqn. (20) into Eqn. (19) yields:

$$\frac{d\,ZEM}{d\,t} = \frac{r^3\omega_s^3}{\dot{r}^2} + \frac{r^2\omega_s}{\dot{r}^2}(a_{tr} - a_{tm}) - \frac{r}{\dot{r}}(a_{t\theta} - a_{m\theta}) \tag{21}$$

Introducing the nominal time-to-go t_{go} given by:

$$t_{go} = \frac{r}{|v_r|} \tag{22}$$

The first time derivative of *ZEM* can be rewritten as:

$$\frac{d\,ZEM}{d\,t} = r\omega_s^3 t_{go}^2 + t_{go}\left[\omega_s t_{go}(a_{tr} - a_{mr}) + (a_{t\theta} - a_{m\theta})\right] \tag{23}$$

This implies that *ZEM* can be reduced by both a_{mr} and $a_{m\theta}$. Moreover, it is clear that the capability of reducing *ZEM* between a_{mr} and $a_{m\theta}$ depends on the coefficient $\omega_s t_{go}$, which is given by:

$$\omega_s t_{go} = -\frac{r\omega_s}{\dot{r}} = \frac{v_\theta}{|v_r|} \tag{24}$$

Eqn. (24) directly induces the following remark.

Remark 1. If $v_\theta > |v_r|$ during engagement, the capability of a_{mr} in reducing *ZEM* is stronger than that of $a_{m\theta}$, and vice versa.

Note that it is desirable to minimise v_θ at the handover from the mid course to the homing phase. Therefore, v_θ is usually smaller than the magnitude of v_r at the beginning of the homing phase. It is worth noting that f $v_\theta > |v_r|$, *ZEM* shown in Eqn. (18) holds:

$$ZEM = -\frac{r^2\omega_s}{\dot{r}} = r\frac{v_\theta}{|v_r|} > r \tag{25}$$

which should be avoided during the engagement.

B. New 3D PPN Development

The principle of PPN is to successfully reduce miss distance by regulating the LOS rate and maintaining negative closing speed. PPN is widely used for the endo-atmospheric interception since its commanded acceleration is set to be vertical to the interceptor's velocity vector. In 2D space, as shown in Fig. 2, the direction perpendicular to the

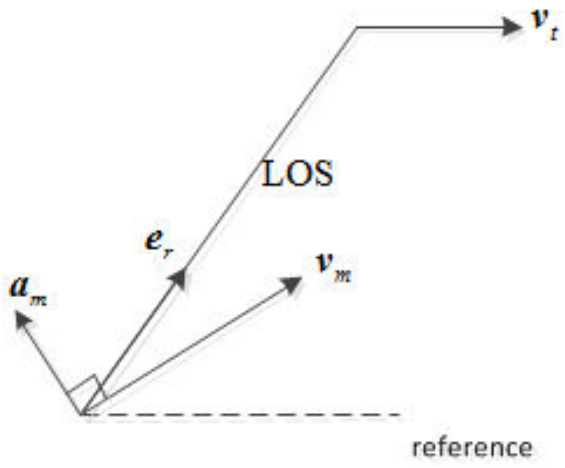

Fig. 2: Two-dimensional engagement geometry

missile velocity vector is unique and consequently the direction of the commanded acceleration can be uniquely determined.

On the other hand, there is a plane that is orthogonal to the missile velocity vector in 3D space. This implies that there are infinite number of vectors that is perpendicular to $\boldsymbol{v}_m$ and hence the direction of the commanded acceleration should be determined. The commanded acceleration of 3D PPN is normally expressed as [1], [15] [17]:

$$\boldsymbol{a}_{PPN} = N\boldsymbol{\omega}_s \times \boldsymbol{v}_m \tag{26}$$

where N denotes the navigation gain, whose value is usually set to be between 3 and 5 in practice. Denoting the direction vector of the missile velocity as $\boldsymbol{t}_m$, the commanded acceleration in conventional 3D PPN is given by:

$$\boldsymbol{a}_{PPN} = Nv_m\omega_s\boldsymbol{e}_\omega \times \boldsymbol{t}_m \tag{27}$$

As shown in Eqn. (27), the direction of the conventional 3D PPN is determined by $\boldsymbol{e}_\omega \times \boldsymbol{t}_m$ which can be expressed as:

$$\boldsymbol{e}_\omega \times \boldsymbol{t}_m = (\boldsymbol{e}_r \times \boldsymbol{e}_\theta) \times \boldsymbol{t}_m = -(\boldsymbol{t}_m \cdot \boldsymbol{e}_\theta)\boldsymbol{e}_r + (\boldsymbol{t}_m \cdot \boldsymbol{e}_r)\boldsymbol{e}_\theta \tag{28}$$

Substituting Eqn. (28) into Eqn. (27) yields:

$$\boldsymbol{a}_{PPN} = Nv_m\omega_s\left[-(\boldsymbol{t}_m \cdot \boldsymbol{e}_\theta)\boldsymbol{e}_r + (\boldsymbol{t}_m \cdot \boldsymbol{e}_r)\boldsymbol{e}_\theta\right] \tag{29}$$

Let us define the direction of the commanded acceleration of the conventional 3D PPN as $\boldsymbol{e}_{PPN}$, i.e.

$$\boldsymbol{e}_{PPN} =: \frac{\boldsymbol{e}_\omega \times \boldsymbol{t}_m}{|\boldsymbol{e}_\omega \times \boldsymbol{t}_m|} \tag{30}$$

From Eqn. (28), it is clear that $\boldsymbol{e}_{PPN}$ is located on the engagement plane which are spanned by $\boldsymbol{e}_r$ and $\boldsymbol{e}_\theta$.

For $v_\theta < |v_r|$, from Remark 1, it is clear that the larger $a_{m\theta}$ is, the more effective the commanded acceleration will be in reducing *ZEM*. Therefore, maximising the projection of the commanded acceleration on the $\boldsymbol{e}_\theta$ axis will make 3D PPN more efficient in reducing *ZEM*. The direction of the acceleration determined by $\boldsymbol{e}_\omega \times \boldsymbol{t}_m$ is not effective in this sense.

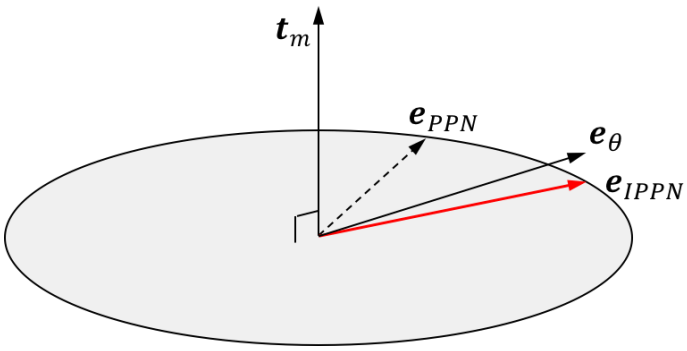

Fig. 3: Geometric relationship of $\boldsymbol{t}_m$, $\boldsymbol{e}_\theta$, $\boldsymbol{e}_{PPN}$, and $\boldsymbol{e}_{IPPN}$: the circle represents the plane perpendicular to $\boldsymbol{t}_m$ and $\boldsymbol{e}_{IPPN}$ must be located in the plane spanned by $\boldsymbol{t}_m$ and $\boldsymbol{e}_\theta$

Now, let us define the optimal direction of the commanded acceleration in 3D PPN as the direction that provides the maximum projection of the acceleration on the $\boldsymbol{e}_\theta$ axis among feasible directions. From Remark 1, it is expected that the optimal direction will provide the strongest capability in reducing *ZEM* at each time step. This optimal direction is denoted as $\boldsymbol{e}_{IPPN}$. For endo-atmospheric interception, the commanded acceleration must be perpendicular to the interceptor's velocity. This means that the set of feasible directions, defined as S_{PPN}, is given by:

$$S_{PPN} = \{\boldsymbol{e}_{PPN} \,|\, \boldsymbol{e}_{PPN} \cdot \boldsymbol{t}_m = 0\} \tag{31}$$

Hence, the optimal direction must also holds the following equality

$$\boldsymbol{e}_{IPPN} \cdot \boldsymbol{t}_m = 0 \tag{32}$$

In order for the maximum projection of the commanded acceleration on $\boldsymbol{e}_\theta$, it is trivial that $\boldsymbol{t}_m$, $\boldsymbol{e}_\theta$ and $\boldsymbol{e}_{IPPN}$ should be located in the same plane. Hence,

$$\boldsymbol{e}_{IPPN} = \frac{\boldsymbol{t}_m \times (\boldsymbol{e}_\theta \times \boldsymbol{t}_m)}{|\boldsymbol{t}_m \times (\boldsymbol{e}_\theta \times \boldsymbol{t}_m)|} = \frac{\boldsymbol{e}_\theta - (\boldsymbol{e}_\theta \cdot \boldsymbol{t}_m)\boldsymbol{t}_m}{\lambda} \tag{33}$$

where:

$$\lambda =: |\boldsymbol{e}_\theta - (\boldsymbol{e}_\theta \cdot \boldsymbol{t}_m)\boldsymbol{t}_m| = \sqrt{1 - (\boldsymbol{e}_\theta \cdot \boldsymbol{t}_m)^2} \tag{34}$$

Fig. 3 depicts the geometric relationship of $\boldsymbol{t}_m$, $\boldsymbol{e}_\theta$, $\boldsymbol{e}_{PPN}$, and $\boldsymbol{e}_{IPPN}$.

As shown in Eqn. (27), the magnitude of the commanded acceleration of conventional 3D PPN becomes smaller as $|\boldsymbol{e}_\omega \times \boldsymbol{t}_m|$ gets smaller. If this happens before the LOS angular speed ω_s being controlled sufficiently small, the commanded acceleration of 3D PPN is not able to effectively stabilise ω_s. Note that this is against the concept of the PPN. Considering this issue and the optimal direction of the commanded acceleration defined, this paper proposed an improved 3D PPN, named IPPN, as:

$$\boldsymbol{a}_{IPPN} = \frac{N v_m \omega_s}{\lambda} \left[\boldsymbol{e}_\theta - (\boldsymbol{e}_\theta \cdot \boldsymbol{t}_m)\boldsymbol{t}_m\right] \tag{35}$$

This proposed approach will enable the commanded acceleration to be applied along the direction where its projection along $\boldsymbol{e}_\theta$ is maximised at each time step. This implies that, in most of practice, the proposed 3D PPN

law can apply more energy on the more effective direction $\boldsymbol{e}_\theta$ in reducing *ZEM*, compared with the conventional 3D PPN.

On the other hand, the magnitude of the acceleration is proportional only to ω_s, i.e.:

$$|\boldsymbol{a}_{IPPN}| = N v_m \omega_s \tag{36}$$

This means that unlike the conventional 3D PN, the LOS angular speed could be more efficiently stabilised even if $|\boldsymbol{e}_\omega \times \boldsymbol{t}_m|$ becomes small.

IV. Analysis

All arguments behind the proposed IPPN algorithm are based on the assumption that v_θ is small enough to hold $v_\theta < |v_r|$. If the assumption is invalid, the proposed guidance algorithm won't be effective. As discussed in Section III-A, it is common that mid course guidance typically aims to minimise v_θ at the hand over to the homing phase. Hence, it is reasonable to assume that the initial value of v_θ in the homing phase is small to satisfy $v_\theta < |v_r|$. To this end, the essential question to be answered is whether or not v_θ can be maintained small enough during the homing phase given a satisfactory initial value.

This section proves that if the navigation gain is properly selected, it is possible to show that v_θ is bounded within a certain range.

Lemma 1. *In addition to A1)-A7), suppose the following two assumptions hold.*

A8) For a constant $\beta \in (0, v_m(1+\rho)]$, the initial value of v_θ satisfy the following condition:

$$v_\theta(t_0) < \beta \tag{37}$$

A9a) N is chosen such that:

$$N > \frac{\dfrac{\alpha r}{\beta v_m} + \rho + \cos\theta_m}{\lambda} \quad \forall t \geq t_0 \tag{38}$$

Then, 3D PPN commanded acceleration defined in Eqn. (26) guarantees that

$$v_\theta(t) < \beta \quad \forall t \geq t_0 \tag{39}$$

Proof. As v_θ is the relative velocity component generating the LOS angular speed ω_s, a Lyapunov-like function, $V(t)$ is defined as:

$$V(t) =: \frac{v_\theta^2(t)}{2} = \frac{[r(t)\omega_s(t)]^2}{2} \tag{40}$$

The first time derivative of the Lyapunov-like function is obtained as:

$$\dot{V} = r\omega_s \left(\dot{r}\omega_s + r\dot{\omega}_s\right) \tag{41}$$

From relative dynamic equations and commanded acceleration, we have:

$$\begin{aligned} r\dot{\omega}_s + 2\dot{r}\omega_s &= a_t \boldsymbol{n}_t \cdot \boldsymbol{e}_\theta - \frac{N v_m \omega_s}{\lambda} \left[\boldsymbol{e}_\theta - (\boldsymbol{e}_\theta \cdot \boldsymbol{t}_m)\, \boldsymbol{t}_m\right] \cdot \boldsymbol{e}_\theta \\ &= a_t \boldsymbol{n}_t \cdot \boldsymbol{e}_\theta - \frac{N v_m \omega_s}{\lambda} \left[1 - (\boldsymbol{e}_\theta \cdot \boldsymbol{t}_m)^2\right] \end{aligned} \tag{42}$$

Considering the definition of λ shown in Eqn. (34), it is clear that:

$$r\dot{\omega}_s + 2\dot{r}\omega_s = a_t \boldsymbol{n}_t \cdot \boldsymbol{e}_\theta - N v_m \omega_s \lambda \tag{43}$$

From Eqn. (16), $\dot{r}\omega_s$ can be written as:

$$\begin{aligned} \dot{r}\omega_s &= v_m \omega_s \left(\rho \boldsymbol{t}_t \cdot \boldsymbol{e}_r - \boldsymbol{t}_m \cdot \boldsymbol{e}_r\right) \\ &= v_m \omega_s \left(\rho \cos\theta_t - \cos\theta_m\right) \end{aligned} \tag{44}$$

Hence:

$$r\dot{\omega}_s + \dot{r}\omega_s = a_t \boldsymbol{n}_t \cdot \boldsymbol{e}_\theta + v_m \omega_s (\cos\theta_m - \rho\cos\theta_t - N\lambda) \tag{45}$$

Substituting Eqn. (45) into Eqn. (41) yields

$$\begin{aligned} \dot{V} &= r\omega_s \left[a_t \boldsymbol{n}_t \cdot \boldsymbol{e}_\theta + v_m \omega_s (\cos\theta_m - \rho\cos\theta_t - N\lambda)\right] \\ &\leq r v_m \omega_s^2 \left(\cos\theta_m + \rho - N\lambda\right) + r\omega_s a_t \end{aligned}$$

From the assumptions A6) and A9e), $\dot{V}$ holds

$$\dot{V} < -\frac{\alpha r^2 \omega_s^2}{\beta} + \alpha r \omega_s = -2\frac{\alpha V}{\beta} + \sqrt{2}\alpha\sqrt{V} \tag{46}$$

Therefore, we have:

$$\sqrt{V}(t) < \frac{\beta}{\sqrt{2}}, \quad \forall t \geq t_0 \tag{47}$$

This proves Eqn. (39) for $t \geq t_0$. □

Lemma 1 implies that, for a missile guided by the proposed IPPN law against an arbitrarily manoeuvring target with limited normal acceleration, v_θ can be bounded in a certain range if the following conditions hold: the initial v_θ is acceptable and the navigation gain is chosen sufficiently large. Eqn. (38) implies that the bigger the speed ratio ρ is, the larger the navigation gain is demanded. It can be also noted that the choice of the navigation gain N depends on the target acceleration bound, not on the entire target acceleration profile.

Remark 2. Lemma 1 also implies that the heading error of IPPN can be bounded. If there is no heading error, i.e. the missile is on collision course, the *vertical relative speed*, v_θ, represented in Eqn. (17) is zero. As the missile speed v_m is not a control variable, the property of the heading error can be investigated by also examining the value of v_θ.

The lower bound of the navigation gain in Lemma 1 is functions of $\cos\theta_m$. Therefore, it is critical to investigate the properties on θ_m. Lemma 2 analyses the range of θ_m against a manoeuvring target.

Lemma 2. *Suppose that the assumptions A1) − A7) hold and the following assumption holds*

A9b) The navigation gain satisfies the following inequality:

$$N > \frac{\lambda}{\cos\theta_m} \tag{48}$$

Then, the commanded acceleration of the IPPN guidance law guarantees θ_m such that:

$$\sin\theta_m(t) \leq \max\left\{\sin\theta_{m0},\ \rho\right\} \quad \Leftrightarrow \quad \cos\theta_m(t) \geq \min\left\{\cos\theta_{m0}, \sqrt{1-\rho^2}\right\}, \quad \forall t \geq t_0 \tag{49}$$

Proof. $\dot{\boldsymbol{t}}_m$ is obtained as:

$$\dot{\boldsymbol{t}}_m = \frac{\boldsymbol{a}_m}{v_m} = \frac{\boldsymbol{a}_{IPPN}}{v_m} = \frac{N\omega_s}{\lambda}\left[\boldsymbol{e}_\theta - (\boldsymbol{e}_\theta \cdot \boldsymbol{t}_m)\,\boldsymbol{t}_m\right], \tag{50}$$

Therefore, we have:

$$\frac{d(\cos\theta_m)}{dt} = -\frac{N\omega_s}{\lambda}(\boldsymbol{e}_\theta \cdot \boldsymbol{t}_m)(\boldsymbol{t}_m \cdot \boldsymbol{e}_r) + \omega_s\,(\boldsymbol{t}_m \cdot \boldsymbol{e}_\theta) \tag{51}$$

Using Eqns. (4) and (17), we can obtain $\boldsymbol{t}_m \cdot \boldsymbol{e}_\theta$ as:

$$\begin{aligned} \boldsymbol{t}_m \cdot \boldsymbol{e}_\theta &= \frac{v_m}{r\omega_s}\,\boldsymbol{t}_m \cdot (\rho\boldsymbol{t} - \boldsymbol{m}) \\ &= \frac{v_m}{r\omega_s}\sin\theta_m\,(\rho\sin\theta_T\cos\Theta - \sin\theta_m) \end{aligned} \tag{52}$$

Substituting Eqn. (52) into Eqn. (51) yield

$$\begin{aligned} \frac{d(\cos\theta_m)}{dt} &= \frac{\omega_s}{\lambda}(\lambda - N\cos\theta_m)\,\boldsymbol{t}_m \cdot \boldsymbol{e}_\theta \\ &= \frac{v_m}{r}(N\cos\theta_m - \lambda)\sin\theta_m\,(\sin\theta_m - \rho\sin\theta_t\cos\Theta) \end{aligned} \tag{53}$$

Since $\theta_m, \theta_t \in [0,\ \pi]$ from their definitions, it is clear that:

$$\frac{d(\cos\theta_m)}{dt} \geq \frac{v_m}{r}(N\cos\theta_m - \lambda)\sin\theta_m\,(\sin\theta_m - \rho\sin\theta_t) \tag{54}$$

Thus, $\dot{\theta}_m$ holds the following inequality:

$$\dot{\theta}_m \leq -\frac{v_m}{r}(N\cos\theta_m - \lambda)\,(\sin\theta_m - \rho\sin\theta_t) \tag{55}$$

Then, for N holding A9c), we have:

$$\begin{cases} \dot{\theta}_m < 0, & \text{if } \sin\theta_m > \rho \\ \dot{\theta}_m \leq 0, & \text{if } \sin\theta_m = \rho \end{cases} \tag{56}$$

This implies that:

$$\sin\theta_m(t) < \sin\theta_{m0}, \quad \forall t \geq t_0, \quad \text{if } \sin\theta_{m0} > \rho \tag{57}$$

Since $\theta_m(t)$ is a continuous function of time unless the relative range becomes zero, Eqn. (56) also means that:

$$\sin\theta_m(t) \leq \rho, \quad \forall t \geq t_0, \quad \text{if } \sin\theta_{m0} \leq \rho \tag{58}$$

Therefore, we have:

$$\sin\theta_m(t) \leq \max\left\{\sin\theta_{m0},\ \rho\right\}, \quad \forall t \geq t_0 \tag{59}$$

It is obvious that the condition in Eqn. (59) is identical to the following condition:

$$\cos\theta_m(t) \geq \min\left\{\cos\theta_{m0}, \sqrt{1-\rho^2}\right\}, \quad \forall t \geq t_0 \tag{60}$$

□

The issue with Lemmas 1 and 2 is that the lower bounds of N are functions of states which are time varying. As it could be practical to determine a value for the navigation gain, it would be beneficial to investigate the upper bound of the bounds of the navigation gain in Lemmas 1 and 2. To do so, it is necessary to first examine the boundedness of λ.

Lemma 3. *Suppose that the assumption A1) – A7) and A9b) satisfy. Then, λ is bounded as:*

$$\min\left\{\cos\theta_{m0}, \sqrt{1-\rho^2}\right\} \leq \lambda \leq 1 \quad \forall t \geq t_0 \tag{61}$$

Proof. From the definition of λ given in Eqn. (34), it is clear that $\lambda \leq 1$. $r\omega_s$ can be rewritten as:

$$r\omega_s = v_m\left(\rho\sin\theta_t - \sin\theta_m\right) \tag{62}$$

Substituting Eqn. (62) into Eqn. (52) yields:

$$\boldsymbol{t}_m \cdot \boldsymbol{e}_\theta = \frac{\sin\theta_m\left(\rho\sin\theta_T\cos\Theta - \sin\theta_m\right)}{\left(\rho\sin\theta_t - \sin\theta_m\right)} \tag{63}$$

Hence, it is trivial that:

$$\boldsymbol{t}_m \cdot \boldsymbol{e}_\theta \leq \sin\theta_m \tag{64}$$

Therefore, we clearly have

$$\lambda \geq \cos\theta_m = \sqrt{1-\sin^2\theta_m} \tag{65}$$

The bound of $\cos\theta_m$, which is given by Eqn. (60) in Lemma 2, completes the proof. □

Now, we can establish the following theorem that provides fixed bounds of the navigation gain.

Theorem 1. *Suppose A1)-A7), A8) hold and the following assumption satisfies. A9c) N is chosen such that*

$$N > \max\left\{\frac{\frac{\alpha r}{\beta v_m} + \rho + \nu}{\nu}, \frac{1}{\nu}\right\} \quad \forall t \geq t_0 \tag{66}$$

where

$$\nu =: \min\{\cos\theta_m\} = \min\left\{\cos\theta_{m0}, \sqrt{1-\rho^2}\right\} \tag{67}$$

Then, Eqn. (39) in Lemma 1 and Eqn. (49) in Lemma 2 hold.

Proof. From Eqn. (65) in Lemma 3, it is trivial that

$$\begin{aligned}\frac{\frac{\alpha r}{\beta v_m} + \rho + \cos\theta_m}{\lambda} &\leq \frac{\frac{\alpha r}{\beta v_m} + \rho + \cos\theta_m}{\cos\theta_m} \\ &\leq \frac{\frac{\alpha r}{\beta v_m} + \rho + \nu}{\nu}\end{aligned} \tag{68}$$

Also, as $\lambda \leq 1$, we have

$$\frac{\lambda}{\cos\theta_m} \leq \frac{1}{\cos\theta_m} \leq \frac{1}{\nu} \tag{69}$$

This means that the navigation meeting assumption A9c) also holds A9a) in Lemma 1 and A9b) in Lemma 2, which completes the proof. □

During the engagement, especially at the homing phase, the initial closing speed is usually smaller than 0 and it is desirable to avoid the situation where $\dot{r}$ becomes positive. Moreover, if 3D PPN maintains negative closing speed over the entire engagement, target interception can be guaranteed. Therefore, the following theorem will briefly

examine the characteristics of the closing speed $\dot{r}$, which is directly related to the capturability, in the new 3D PPN law.

Theorem 2. *Suppose that assumptions A1) − A7) and A9b) are satisfied, $\dot{r}(t_0) < 0$ and the following initial condition is met:*

A10)

$$\cos\theta_{m0} > \max\left\{\rho, \sqrt{1-\rho^2}\right\} \tag{70}$$

Then, $\dot{r}(t) < 0$ for all $t \geq t_0$.

Proof. For $\rho < 1/\sqrt{2}$, Lemma 2 and Eqn. (70) imply that

$$\begin{aligned} \cos\theta_m(t) &\geq \min\left\{\cos\theta_{m0}, \sqrt{1-\rho^2}\right\} \\ &\geq \sqrt{1-\rho^2}, \quad \forall t \geq t_0 \end{aligned} \tag{71}$$

Then, given $\rho < 1/\sqrt{2}$, the closing speed holds the following condition:

$$\begin{aligned} \dot{r}(t) &= v_m\omega_s\left(\rho\cos\theta_t - \cos\theta_m\right) \\ &\leq v_m\left(\rho - \sqrt{1-\rho^2}\right) < 0, \quad \forall t \geq t_0 \end{aligned} \tag{72}$$

In case of $\rho \in [1/\sqrt{2},\ 1)$, it is clear from the initial conditions given in Eqn. (70) and Lemma 2 that $\cos\theta_m(t) > \rho$ for all $t \geq t_0$. Hence, $\dot{r}(t)$ holds:

$$\dot{r}(t) < v_m\left(\rho - \rho\right) = 0, \quad \forall t \geq t_0 \tag{73}$$

□

Remark 3. Given $\dot{r} \leq 0$ for all $t \geq t_0$, we have

$$\max\left\{\frac{\frac{\alpha r}{\beta v_m} + \rho + \nu}{\nu}, \frac{1}{\nu}\right\} \leq \max\left\{\frac{\frac{\alpha r_0}{\beta v_m} + \rho + \nu}{\nu}, \frac{1}{\nu}\right\} \tag{74}$$

The value of the upper bound given in Eqn. (74) is determined by the fixed values of parameters and the initial values of some states. Therefore, from Theorem 1, it is clear that the lower bound of the navigation gain can be determined by a fixed value at the beginning of the engagement.

Remark 4. The capturability condition of A10) is conservative: the condition implies that the missile flies towards to the target at the beginning of homing. Note that it is straightforward to find more general condition following [18] or [20]. However, since this is not the main scope of this study and derivation becomes lengthy, we limit our discussion on the capturability to Theorem 2.

V. Numerical Simulations

This section validates the performance of the proposed IPPN against the typical 3D PPN via numerical simulations. Since the proposed guidance is for the homing phase, this section considers only engagement scenarios in the homing phase. The maximum acceleration of the missile is assumed to be bounded to $\pm 20\ g$ where $g \approx 9.81\ m/s^2$. Table I provides the initial simulation conditions.

TABLE I: Simulation conditions

	Value
Initial missile position	$(0,\ 0,\ 0)$ km
Initial relative distance	3 km
Initial heading angle	5 deg
Missile speed	800 m/s
Target speed	700 m/s
Initial LOS elevation angle	60 deg
Initial LOS azimuth angle	30 deg
Initial target pitch angle	0 deg
Initial target yaw angle	135 deg

We consider two cases in which target acceleration profiles are different, but the other engagement conditions remain the same. The target acceleration profile in the first case is given as:

$$\boldsymbol{a}_t = \begin{cases} 5g\frac{\boldsymbol{i}_B \times \boldsymbol{v}_t}{|\boldsymbol{i}_B \times \boldsymbol{v}_t|}, & \text{for } t \in [0,\ 1.5]sec \\ 5g\frac{\boldsymbol{j}_B \times \boldsymbol{v}_t}{|\boldsymbol{j}_B \times \boldsymbol{v}_t|}, & \text{for } t > 1.5sec \end{cases} \tag{75}$$

where $\boldsymbol{i}_B$ and $\boldsymbol{j}_B$ denote the unit vectors corresponding to x and y axes in the body coordinate system, and g gravity, i.e., $g \approx 9.81 m/sec^2$. The upper bound of the target acceleration, α, is estimated as $5g$. In the second case, the actual acceleration is assumed to exceed the estimated upper bound, i.e.:

$$\boldsymbol{a}_t = \begin{cases} 5g\frac{\boldsymbol{i}_B \times \boldsymbol{v}_t}{|\boldsymbol{i}_B \times \boldsymbol{v}_t|}, & \text{for } t \in [0,\ 1.5]sec \\ 15g\frac{\boldsymbol{j}_B \times \boldsymbol{v}_t}{|\boldsymbol{j}_B \times \boldsymbol{v}_t|}, & \text{for } t > 1.5sec \end{cases} \tag{76}$$

The second case is considered to demonstrate clear performance difference between typical PPN and the proposed IPPN.

It is assumed that the mid course guidance achieves the initial v_θ at the hand-over to the terminal homing smaller or equal to $100 m/s$. Hence, β in Eqn. (37) is set to be 100. Note that the initial v_θ is $71.8294 m/s$. Given the initial engagement conditions and parameter values, we obtain:

$$\max\left\{\frac{\frac{\alpha r_0}{\beta v_m} + \rho + \nu}{\nu}, \frac{1}{\nu}\right\} = 4.9148$$

Following Theorem 1 and Remark 3, we set $N = 5$ for IPPN. For fair comparison, the navigation for the conventional 3D PPN is also set to be equal to 5.

Simulation results in case 1 are shown in Fig. 4. The time histories of total commanded acceleration and the angular speed of the LOS vector are depicted in Figs. 4a and 4b, respectively. The magnitude of the commanded acceleration of conventional 3D PPN becomes smaller as $|\boldsymbol{e}_\omega \times \boldsymbol{t}_m|$ gets smaller before the LOS angular speed ω_s being sufficiently controlled. Hence, the commanded acceleration of 3D PPN is not able to effectively stabilise ω_s. As ω_s does not remain small, the velocity ratio described in Eqn. (24) and the total commanded acceleration become larger. Given this condition, Eqn. (23) indicates that *ZEM* can be still controlled in PPN, but not as efficient

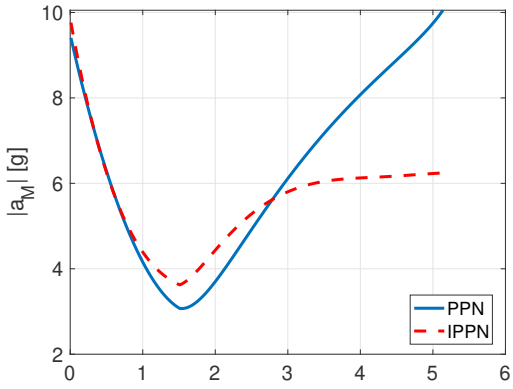

(a) Total commanded acceleration

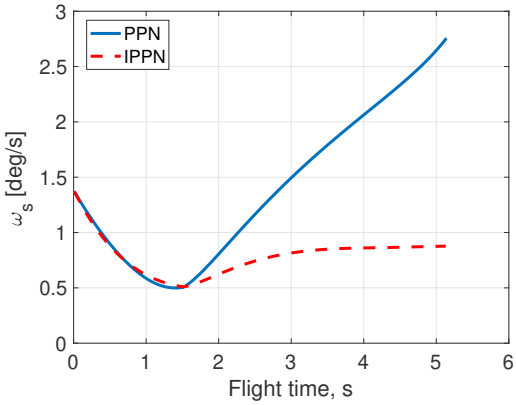

(b) Angular speed of the LOS vector

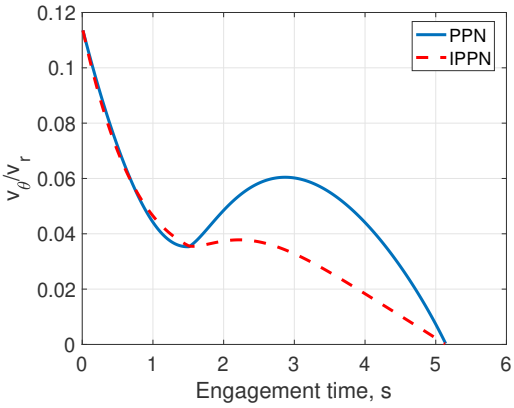

(c) Speed ratio

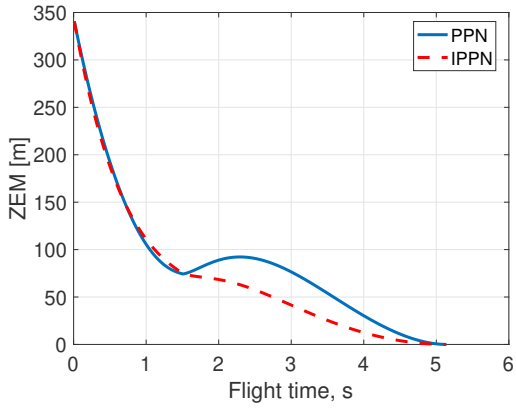

(d) *ZEM*

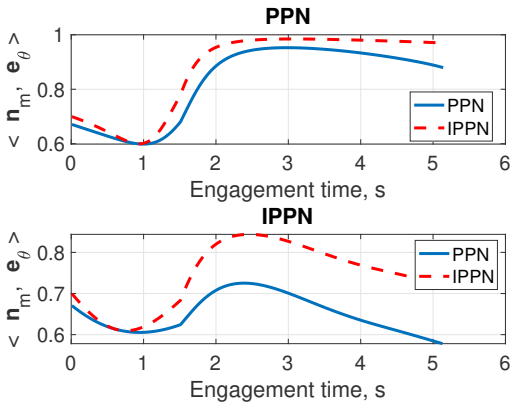

(e) $< \boldsymbol{n}_m, \boldsymbol{e}_\theta >$

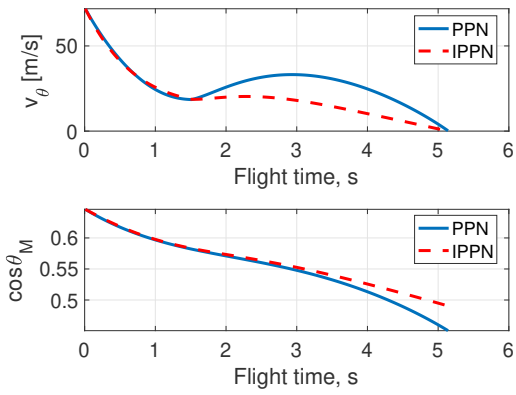

(f) v_θ and $\cos\theta_m$

Fig. 4: Simulation results in Case 1: $\boldsymbol{n}_m$ is the unit vector along the commended acceleration vector of the missile

as IPPN. This is confirmed in Fig. 4a. The simulation results confirm that IPPN can more effectively stabilise ω_s and the total commanded acceleration than 3D PPN. This is desirable in terms of robustness against potential uncertainties, disturbances and/or noises.

As illustrated in Fig. 4c, the speed ratio v_θ/v_r is decreasing over the engagement. When the ratio became significantly small at around $1.5\ sec$, the proposed IPPN algorithm can reduce the ratio in a more efficient way, compared with PPN. Fig. 4d demonstrates that the profiles of *ZEM* follows a similar pattern as the speed ratio. As shown in Fig. 4a, the conventional PPN applies more energy to reduce both the speed ratio and *ZEM*. Note that, the final miss distance of PPN is $2.2639\ m$ and that of IPPN is $0.2668\ m$ in case 1. This confirms that IPPN can reduce *ZEM* in a more efficient way than PPN.

The projection of the commanded acceleration can be examined by checking $< \boldsymbol{n}_m, \boldsymbol{e}_\theta >$ where $<,>$ denotes the vector inner product and $\boldsymbol{n}_m$ is the unit vector along the commended acceleration vector of the missile. As discussed, the commanded acceleration in the proposed IPPN is applied along the direction where its projection along $\boldsymbol{e}_\theta$ is maximised. This enables the application of the commanded acceleration to a direction, more effectively reducing *ZEM*, compared with the conventional 3D PPN. The profiles of the inner product are shown in Fig. 4e. Since the engagement conditions become completely different once the two different guidance algorithms start to be implemented, direct comparison on the inner product is not fair. For fair comparison, we fix a guidance algorithm applied and check the inner product in PPN and IPPN. The figure above in Fig. 4e is the case where the guidance algorithm applied is PPN. The figure below in Fig. 4e is the case where IPPN is applied. As shown in Fig. 4e, IPPN produces always bigger $< \boldsymbol{n}_m, \boldsymbol{e}_\theta >$, compared with the conventional 3D PPN. This means that the proposed IPPN algorithm can reduce *ZEM* in a more efficient way, which are confirmed from Figs 4a–4d.

Fig. 4f shows time histories of v_θ and $\cos\theta_m$. The navigation gain is selected to satisfy the condition given in Theorem 1. Hence, Lemma 1 implies that $v_\theta < \beta$ for all $t \geq 0$, which is confirmed by the figure above in Fig. 4f. Also, from Lemma 2, $\cos\theta_m(t) \geq \min\left\{\cos\theta_{m0}, \sqrt{1-\rho^2}\right\}$ for all $t \geq 0$. This implies that as $\min\left\{\cos\theta_{m0}, \sqrt{1-\rho^2}\right\} = 0.6614$, $\cos\theta_m(t) \geq 0.6614$. This is consistent with the result shown in the figure at the bottom in Fig. 4f. The simulation results confirm the analysis results in Section IV.

In case 2, the actual maximum target acceleration α is $15\ g$ and hence the actual bound of the navigation gain is

$$\max\left\{\frac{\frac{\alpha r_0}{\beta v_m}+\rho+\nu}{\nu}, \frac{1}{\nu}\right\} = 10.4765$$

However, as discussed, the navigation gain is selected as 5. The simulation results in case 2 are depicted in Fig. 5. The order of the sub-figures in Fig. 5 is the same as that in Fig. 4. The results shown in Figs. 5a – 5e confirm that the proposed IPPN can efficiently reduce *ZEM* to zero. In the conventional 3D PPN fails, the commanded acceleration reaches to the maximum bound and fails to successfully reduce *ZEM*. Consequently, the PPN algorithm fails to intercept the target where as the proposed IPPN successfully intercepts the target: the minimum miss distance is $74.0499\ m$ and 1.5182 in PPN and IPPN, respectively. As illustrated in Fig. 4e, $< \boldsymbol{n}_m, \boldsymbol{e}_\theta >$ is always larger in IPPN than in PPN. As discussed in Section III, this the main enabler of the efficient reduction of *ZEM* and consequently interception of the target. Although the navigation gain in IPPN didn't meet the condition given by

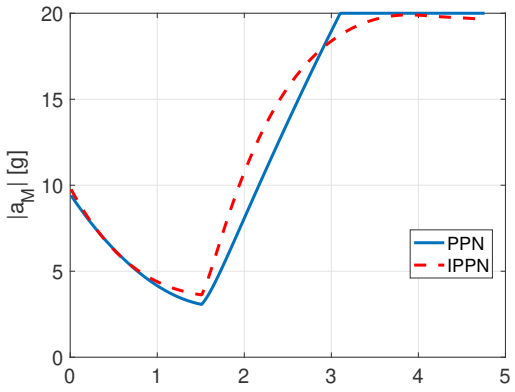

(a) Total commanded acceleration

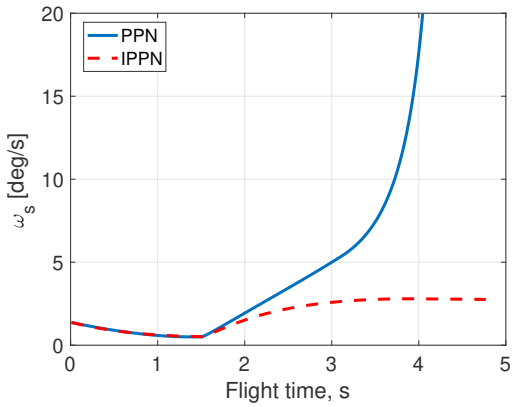

(b) Angular speed of the LOS vector

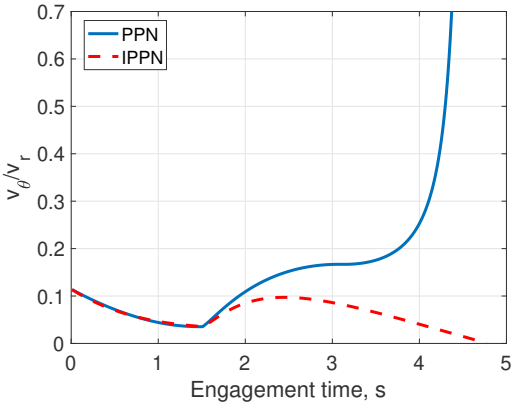

(c) Speed ratio

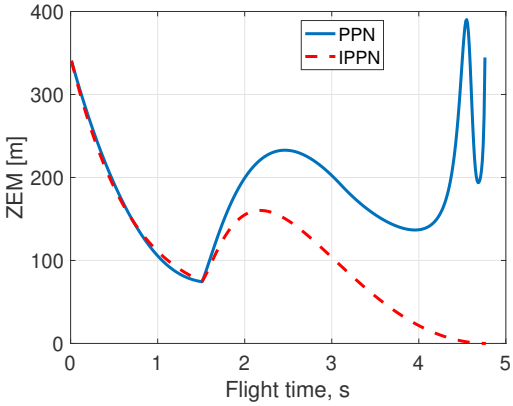

(d) *ZEM*

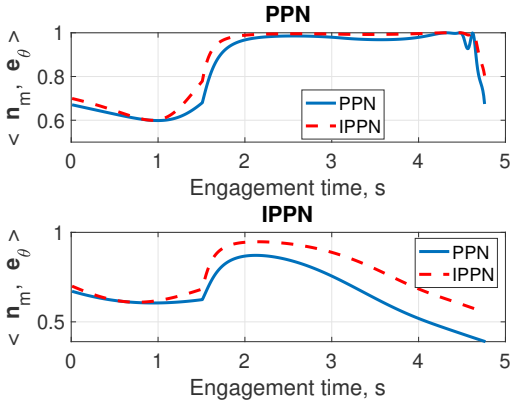

(e) $< \boldsymbol{n}_m, \boldsymbol{e}_\theta >$

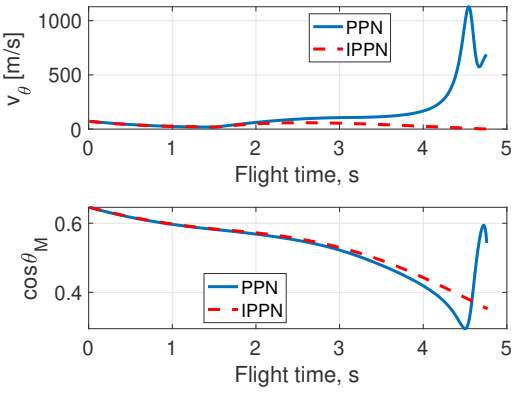

(f) v_θ and $\cos\theta_m$

Fig. 5: Simulation results in Case 2: $\boldsymbol{n}_m$ is the unit vector along the commended acceleration vector of the missile

Eqn. (74) in Theorem 1, IPPN satisfies the bound condition of v_θ and $\cos\theta_m$ provided in Lemmas 1 and 2. This implies that the actual bound of the navigation gain should be tighter and finding the tighter bound could be subject of future study. Note that PPN cannot bound v_θ and $\cos\theta$ in case 2, unlike IPPN.

VI. Conclusions

This paper suggests that determination of the commanded acceleration vector, i.e. magnitude and direction, can significantly improve the performance of endo-atmospheric interception against manoeuvring targets in 3D space. For the validation of the suggestion, this paper conducts analysis of relative motion between the interceptor and target in 3D space. The analysis confirms that there exists a direction which is more efficient in reducing the *zero-effort miss (ZEM)* and consequently in improving guidance performance. Based on the analysis, this paper proposes a new 3D pure proportional navigation (PPN) guidance law which adapts the efficient direction found for the direction of the commanded acceleration. Note that the new algorithm developed is called Improved PPN (IPPN). Unlike traditional 3D PPN, IPPN maintains the guidance command proportional only to the LOS rate. The validity of the main arguments of the paper is investigated by theoretical analysis. The analysis provides bounds of the navigation gain that hold the validity of the main arguments. The performance of the proposed algorithm is examined and compared with that of traditional 3D PPN via numerical simulations. The simulation results confirm the analysis results and outperformance of the new guidance algorithm over traditional 3D PPN. It is worth noting that the effective direction identified is not constrained by a specific type of guidance algorithms, but valid for any type of guidance algorithms. Therefore, it could be applicable to most of existing modern guidance laws: the efficient direction could be directly integrated with their original guidance command formations. Thorough investigation on such integration and corresponding performance improvement is subject to future research.

References

[1] F. P. Adler, "Missile guidance by three-dimensional proportional navigation," *Journal of Applied Physics*, vol. 27, no. 5, pp. 500–507, 1956.

[2] K. Becker, "Closed-form solution of pure proportional navigation," *Aerospace and Electronic Systems, IEEE Transactions on*, vol. 26, no. 3, pp. 526–533, 1990.

[3] M. Guelman, "A qualitative study of proportional navigation," *IEEE Transactions on Aerospace and Electronic Systems*, vol. 4, no. AES-7, pp. 637–643, 1971.

[4] U. Shukla and P. Mahapatra, "Generalized linear solution of proportional navigation," *Aerospace and Electronic Systems, IEEE Transactions on*, vol. 24, no. 3, pp. 231–238, 1988.

[5] F. Tyan, "Analysis of ppn guidance law-a new approach," in *American Control Conference (ACC), 2013*. IEEE, 2013, pp. 1030–1035.

[6] ——, "Analysis of 3d ppn guidance laws for nonmaneuvering target," *IEEE Transactions on Aerospace and Electronic Systems*, vol. 51, no. 4, pp. 2932–2943, 2015.

[7] K.-B. Li, W.-S. Su, and L. Chen, "Performance analysis of realistic true proportional navigation against maneuvering targets using lyapunov-like approach," *Aerospace Science and Technology*, vol. 69, pp. 333–341, 2017.

[8] K. Li, Y. Liang, W. Su, and L. Chen, "Performance of 3d tpn against true-arbitrarily maneuvering target for exoatmospheric interception," *Science China Technological Sciences*, vol. 61, no. 8, pp. 1161–1174, 2018. [Online]. Available: https://doi.org/10.1007/s11431-018-9310-5

[9] P.-J. Yuan and J.-S. Chern, "Solutions of true proportional navigation for maneuvering and nonmaneuvering targets," *Journal of Guidance, Control, and Dynamics*, vol. 15, no. 1, pp. 268–271, 1992.

[10] H. M. Prasanna and D. Ghose, "Retro-proportional-navigation: A new guidance law for interception of high speed targets," *Journal of Guidance, Control, and Dynamics*, vol. 35, no. 2, pp. 377–386, 2012. [Online]. Available: https://doi.org/10.2514/1.54892

[11] M. Guelman, "Missile acceleration in proportional navigation," *IEEE Transactions on Aerospace and Electronic Systems*, vol. 3, no. AES-9, pp. 462–463, 1973.

[12] Y. B. Shtessel, I. A. Shkolnikov, and A. Levant, "Guidance and control of missile interceptor using second-order sliding modes," *Aerospace and Electronic Systems, IEEE Transactions on*, vol. 45, no. 1, pp. 110–124, 2009.

[13] M. Guelman, "Proportional navigation with a maneuvering target," *IEEE Transactions on Aerospace and Electronic Systems*, vol. 3, no. AES-8, pp. 364–371, 1972.

[14] S. Ghawghawe and D. Ghose, "Pure proportional navigation against time-varying target manoeuvres," *Aerospace and Electronic Systems, IEEE Transactions on*, vol. 32, no. 4, pp. 1336–1347, 1996.

[15] I.-J. Ha, J.-S. Hur, M.-S. Ko, and T.-l. Song, "Performance analysis of png laws for randomly maneuvering targets," *Aerospace and Electronic Systems, IEEE Transactions on*, vol. 26, no. 5, pp. 713–721, 1990.

[16] B. S. Kim, J. G. Lee, and H. S. Han, "Biased png law for impact with angular constraint," *Aerospace and Electronic Systems, IEEE Transactions on*, vol. 34, no. 1, pp. 277–288, 1998.

[17] S. H. Song and I. J. Ha, "A lyapunov-like approach to performance analysis of 3-dimensional pure png laws," *Aerospace and Electronic Systems, IEEE Transactions on*, vol. 30, no. 1, pp. 238–248, 1994.

[18] J.-H. Oh and I.-J. Ha, "Capturability of the 3-dimensional pure png law," *Aerospace and Electronic Systems, IEEE Transactions on*, vol. 35, no. 2, pp. 491–503, 1999.

[19] J.-H. Oh, "Solving a nonlinear output regulation problem: zero miss distance of pure png," *IEEE transactions on automatic control*, vol. 47, no. 1, pp. 169–173, 2002.

[20] K. Li, H.-S. Shin, A. Tsourdos, and M.-J. Tahk, "Capturability of 3d ppn against lower-speed maneuvering target for homing phase," *IEEE Transactions on Aerospace and Electronic Systems*, vol. PP, pp. 1–1, 08 2019.

[21] S. He and C.-H. Lee, "Optimality of error dynamics in missile guidance problems," *Journal of Guidance, Control, and Dynamics*, vol. 41, no. 7, pp. 1624–1633, 2018. [Online]. Available: https://doi.org/10.2514/1.G003343

[22] ——, "Optimal impact angle guidance for exo-atmospheric interception utilizing gravitational effect," *IEEE Transactions on Aerospace and Electronic Systems*, vol. PP, pp. 1–1, 09 2018.

[23] S. He, D. Lin, and J. Wang, "Continuous second-order sliding mode based impact angle guidance law," *Aerospace Science and Technology*, vol. 41, pp. 199–208, 2015.

[24] ——, "Integral global sliding mode guidance for impact angle control," *IEEE Transactions on Aerospace and Electronic Systems*, vol. 55, no. 4, pp. 1843–1849, 2018.

[25] D. Zhou, S. Sun, and K. L. Teo, "Guidance laws with finite time convergence," *Journal of guidance, control, and dynamics*, vol. 32, no. 6, pp. 1838–1846, 2009.

[26] H.-S. Shin, A. Tsourdos, and K.-B. Li, "A new three-dimensional sliding mode guidance law variation with finite time convergence," *IEEE Transactions on Aerospace and Electronic Systems*, vol. 53, no. 5, pp. 2221–2232, 2017.

[27] K. Li, H.-S. Shin, and A. Tsourdos, "Capturability of a sliding mode guidance law with finite time convergence," *IEEE Transactions on Aerospace and Electronic Systems*, vol. PP, pp. 1–1, 10 2019.

[28] V. Shaferman and Y. Oshman, "Cooperative interception in a multi-missile engagement," in *Proceedings of AIAA Gudance, Navigation, and Control Conference and Exhibit*, Chicago, Illinois, USA, 2009.

[29] S. Y. Hayoun, M. Weiss, and T. Shima, "A mixed l 2/lα differential game approach to pursuit-evasion guidance," *IEEE Transactions on Aerospace and Electronic Systems*, vol. 52, no. 6, pp. 2775–2788, 2016.

[30] S. He and D. Lin, "Three-dimensional optimal impact time guidance for antiship missiles," *Journal of Guidance, Control, and Dynamics*, vol. 42, no. 4, pp. 941–948, 2019.

[31] Y.-C. Chiou and C.-Y. Kuo, "Geometric approach to three-dimensional missile guidance problem," *Journal of Guidance, Control, and Dynamics*, vol. 21, no. 2, pp. 335–341, 1998. [Online]. Available: https://doi.org/10.2514/2.4240

[32] B. A. White, R. Zibkowski, and A. Tsourdos, "Direct intercept guidance using differential geometry concepts," *IEEE Transactions on Aerospace and Electronic Systems*, vol. 43(3), pp. 899–919, 2007.

[33] K. Li, W. Su, and L. Chen, "Performance analysis of three-dimensional differential geometric guidance law against low-speed maneuvering targets," *Astrodynamics*, vol. 2, no. 3, pp. 233–247, 2018.

[34] P. Wang, Y. Guo, G. Ma, and B. Wie, "New differential geometric guidance strategies for impact-time control problem," *Journal of Guidance, Control, and Dynamics*, vol. 42, no. 9, pp. 1982–1992, 2019.

[35] K. Li, T. Zhang, and L. Chen, "Ideal proportional navigation for exoatmospheric interception," *Chinese Journal of Aeronautics*, vol. 26, no. 4, pp. 976–985, 2013.

[36] K. Li, L. Chen, and G. Tang, "Improved differential geometric guidance commands for endoatmospheric interception of high-speed targets," *Science China Technological Sciences*, vol. 56, no. 2, pp. 518–528, 2013.

[37] N. A. Shneydor, *Missile guidance and pursuit: kinematics, dynamics and control*. Elsevier, 1998.

Hyo-Sang Shin received his BSc from Pusan National University in 2004 and gained an MSc on flight dynamics, guidance and control in Aerospace Engineering from KAIST and a PhD on cooperative missile guidance from Cranfield University in 2006 and 2010, respectively. He is currently a Professor of Guidance, Control and Navigation (GNC) Systems in Autonomous and Intelligent Systems Group at Cranfield University. His current research interests include multiple target tracking, adaptive and sensor-based control, data-centric GNC, and distributed control of multiple agent systems.

Ke-Bo Li received the B.S. degree in Aerospace Engineering and the M.S. and Ph.D. degrees on Flight Vehicle Design in Aeronautical and Astronautical Science and Technology from National University of Defense Technology (NUDT), Changsha, China, in 2008, 2010, and 2016, respectively. Now, he is an Associate Professor in Department of Applied Mechanics, College of Aerospace Science and Engineering, NUDT. His main research interests include: 1) missile guidance laws; 2) spacecraft guidance and control.

2021-03-23

An improvement in three-dimensional pure proportional navigation guidance

Shin, Hyo-Sang

IEEE

Shin H-S, Li K-B. (2021) An improvement in three-dimensional pure proportional navigation guidance. IEEE Transactions on Aerospace and Electronic Systems, Volume 57, Number 5, October 2021, pp. 3004-3014

https://doi.org/10.1109/TAES.2021.3067656